Linear State Load Estimators for a PMSM system

Barna Temesi

Abstract—This short design documentation presents the used system model, parameters and load observer. The used observers are a Luenberger observer and a Kalman-filter. The estimated signal is then used for feedforward compensation.

Index Terms: dynamic modelling of syncronous motors, *dq*-reference frame, PMSM, Load torque estimation, Luenberger observer, Kalman-filter, Optimal state estimation

◆

1 INTRODUCTION

As in every design process, after the problem statement, the system has to be modeled and analyzed. This starts with an overview of the motor parameters. Next, the motor voltage equations, which are already given in the dq-reference frame, are examined. The mechanical equation of the motor is also presented.

This documentation does not consider the FOC used in the system. The focus is strictly on the load torque estimators and feed-forward load torque compensation.

The load torque estimator is based on the thesis: [1]. The original paper is the next: [5]. The Kalman-filter is obviously based on the marvelous book of: [6].

2 MODEL OF THE SYSTEM

The motor, in the scope of this thesis, is an SPMSM. This means that the permanent magnets are located on the surface of the rotor. Due to this, the motor is non-salient, and also the reluctance path is equal on the d- and q-axis. This results in equal inductance on the d- and q-axis. For easier understanding, the machine inductance will be denoted as L_s [2].

$$L_d = L_q = L_s \qquad (1)$$

The most important parameters of the motor and the other necessary system parameters are listed in the table 1.
As can be seen from the table, the motor has 4 pole pairs. Generally speaking, this means that the machine is more geared towards high-speed operation. In high-torque operation applications, like in the case of a steering motor, the number of poles might exceed a 100.
In simulations, the total system resistance will be used, which takes into account the resistance of every possible component in the setup [1].

Table 1: *System parameters, from previous projects such as*

Description	Notation	Value	Unit
Number of pole pairs	N_{pp}	4	-
Winding resistance	R_w	0.19	Ω
Total system resistance	R_s	0.268	Ω
q and d-axis inductance	L_m	2.2	mH
Rotor PM flux linkage	λ_{mpm}	0.12258	wB
Rated speed, SPMSM	$\omega_{m,rated}$	4500	rpm
Rated torque, SPMSM	$\tau_{m,rated}$	20	Nm
Rated power, SPMSM	$P_{m,rated}$	9.4	kW
Rated speed, IM	$\omega_{IM,rated}$	1400	rpm
Rated torque, IM	$\tau_{IM,rated}$	14	Nm
Rated power, IM	$P_{IM,rated}$	2.2	kW
Rated current, VSI	I_{VSI}	35	A
IM machine inertia	J_{IM}	0.0069	$kg \cdot m^2$
SPMSM machine inertia	J_{SPMSM}	0.0048	$kg \cdot m^2$
Total system inertia	J_{sys}	0.0146	$kg \cdot m^2$
Coulomb friction	C	0.2295	Nm
Viscous friction	B	0.0016655	N

The motor voltage equations are shown in equation (2). Due to the assumption that the system is symmetrical and balanced, the zero term (v_0) is zero.

$$
\begin{aligned}
v_d &= R_s i_d + p\lambda_d - \omega_r \lambda_q \\
v_q &= R_s i_q + p\lambda_q + \omega_r \lambda_d \\
v_0 &= 0
\end{aligned}
\qquad (2)
$$

In the abc-reference frame, the machine flux-linkage is dependent on position and the machine inductance is constant for a non-salient pole machine, but because the model is already transformed into the $dq0$-reference frame, the machine inductance is constant.

The stator $dq0$-reference frame is aligned with the rotor reference frame, which is naturally in the $dq0$-reference frame. The rotor d-axis is chosen to be aligned with the maximum flux density line at no load condition. The q-axis is always leading the d-axis by 90 degrees electric. This way, it is aligned with the minimum flux density line [1].
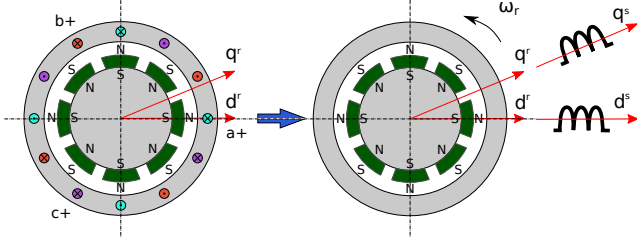
Figure 1: *Reference frame transformation from **abc** to dq. The structure of the motor is also shown. Inspiration: [4]*

The two d-axis is in line now. This is convenient because, it results in the d-axis and the q-axis flux-linkage as shown in equation (3).

$$\lambda_d = (L_{ls} + L_{md})\, i_d + \lambda_{mpm} = L_d i_d + \lambda_{mpm} \qquad (3)$$
$$\lambda_q = (L_{ls} + L_{mq}) = L_q i_q$$
$$\lambda_0 = 0$$

After substitution, the voltage equations may be rewritten as seen in equation (4).

$$v_d = R_s i_d + p(L_d i_d + \lambda_{mpm}) - \omega_r L_q i_q \qquad (4)$$
$$v_q = R_s i_q + p(L_q i_q) + \omega_r(L_d i_d + \lambda_{mpm})$$

Where p is the differential operator $\frac{d}{dt}$. Differentiating the equation, keeping in mind that the derivative of a constant is zero, will result in the following.

$$v_d = R_s i_d + L_d p i_d - \omega_r L_q i_q \qquad (5)$$
$$v_q = R_s i_q + L_q p i_q + \omega_r(L_d i_d + \lambda_{mpm})$$

In one more step, the homogeneous first-order differential equation of the system is acquired.

$$\frac{d}{dt} i_d = -\frac{R_s}{L_d} i_d + \frac{1}{L_d} v_d + \omega_r \frac{L_q}{L_d} i_q \qquad (6)$$
$$\frac{d}{dt} i_q = -\frac{R_s}{L_q} i_q + \frac{1}{L_q} v_q - \omega_r \frac{L_d}{L_q} i_d - \frac{1}{L_q} \omega_r \lambda_{mpm}$$

Equations (4) also contain the back-EMF voltage components which are very important in position estimation, hence they are highlighted here:

$$e_d = -\omega_r L_q i_q \qquad (7)$$
$$e_q = \omega_r(L_d i_d + \lambda_{mpm})$$

The governing torque equation can be derived from the equation of the input power of the windings. Simplifying this equation, using the attributions of the SPMSM machine, yields the following expression:

$$T_e = \frac{3}{2} N_{pp} (\lambda_d i_q - \lambda_q i_d) \qquad (8)$$

$$T_e = \frac{3}{2} \frac{N_{poles}}{2} (\lambda_{mpm} i_q + (L_d - L_q) i_d i_q) \qquad (9)$$

$$T_e = \frac{3}{2} N_{pp} (\lambda_{mpm} i_q) \qquad (10)$$

Using Newton's second law, the mechanical equation of the system can be derived as shown in equation (11) [1].

$$T_e = j_{red} \frac{d\omega_m}{dt} + B_{m,red} \omega_m + T_{dist} \qquad (11)$$

Where J is the total system inertia and T_{dist}, the disturbance torque, consists of the load torque and Coulomb friction. The total system inertia includes the inertia of both the IM and PMSM machine and also the coupling and fastening components between them.

The first term is related to the torque needed to accelerate the system without friction, the last two terms are related to the torque which is needed to overcome the viscous friction and the disturbance torque, respectively.

3 LOAD TORQUE IDENTIFICATION (LTID)

The steps of the design of the observer are presented in this section.

Start by deriving the mechanical equation of the system using Newton's 2_{nd} law. This is shown in equations (12), (13).

$$j_{red} \dot{\omega}_m = \sum T_{sum} \qquad (12)$$

$$\dot{\omega}_m = \frac{1}{j_{red}} \sum T_{sum} \qquad (13)$$

Detail this, such as:

$$j_{red} \dot{\omega}_m = T_m - T_{load} - B_{m,red} \omega_m - T_{dist,residual} \qquad (14)$$

Where, the actuator dynamics are shown in (15). The actuator dynamics were reduced to first-order.

$$\dot{T}_m = \frac{1}{\tau_m} (T_{m,ref} - T_m) \qquad (15)$$

The modified system structure is depicted on figure 2. The feed-forward compensation helps with the transient response and disturbance rejection of the control system.
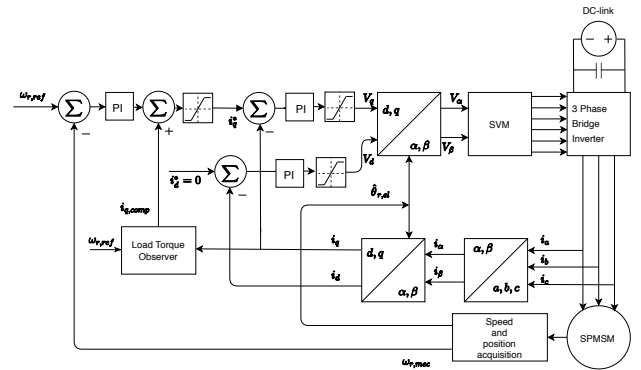

Figure 2: *Block diagram of the system with a load torque observer*

3.1 Luenberger Observer

A linear state observer is constructed based on the mechanical equation of the system. The standard state-space form is presented in (16).

$$\dot{\boldsymbol{x}} = A\boldsymbol{x} + B\boldsymbol{u} + Gw$$
$$\boldsymbol{y} = C\boldsymbol{x} + D\boldsymbol{u} + \nu \tag{16}$$

First, the state-space representation of the system is established in equations (17), (18). The load is already transformed to be a state. The input u is the actual motor torque T_m.

$$\begin{bmatrix} \dot{\omega}_m \\ \dot{T}_{load} \end{bmatrix} = \begin{bmatrix} -\frac{B_{m,red}}{j_{red}} & -\frac{1}{j_{red}} \\ 0 & \tau_{load} \end{bmatrix} \begin{bmatrix} \omega_m \\ T_{load} \end{bmatrix} + \begin{bmatrix} \frac{1}{j_{red}} \\ 0 \end{bmatrix}$$
$$T_m + \begin{bmatrix} 1 & 0 \\ 0 & 1 \end{bmatrix} \begin{bmatrix} w_{MotSpd} \\ w_{dist,load} \end{bmatrix} \tag{17}$$

$$\omega_m = \begin{bmatrix} 1 & 0 \end{bmatrix} \begin{bmatrix} \omega_m \\ T_{load} \end{bmatrix} + \nu_{MotSpd} \tag{18}$$

Where, τ_{load} is either -1/1000 or 0, and $D = 0$.

Before designing the state observer, the observability of the second-order system has to be checked. The observability matrix is shown in equation (19).

$$\boldsymbol{Ob} = \begin{bmatrix} C \\ CA \end{bmatrix} \tag{19}$$

The matrix is full rank, therefore the system is observable. Utilizing linear control theory, a linear state observer can be designed [5], [6]. This is presented in equations (20).

$$\dot{\hat{\boldsymbol{x}}} = A\hat{\boldsymbol{x}} + B\boldsymbol{u} + \boldsymbol{L}[\boldsymbol{y} - C\hat{\boldsymbol{x}}]$$
$$\dot{\hat{\boldsymbol{x}}} = (A - LC)\hat{\boldsymbol{x}} + \begin{bmatrix} B & \boldsymbol{L} \end{bmatrix} \begin{bmatrix} u \\ y \end{bmatrix} \tag{20}$$
$$\hat{\boldsymbol{y}} = C\hat{\boldsymbol{x}}$$

The equation states that, by designing the observer gains ($\boldsymbol{L} = [l_1; l_2]$) to make the new system ($\boldsymbol{A} - \boldsymbol{LC}$) stable and sufficiently fast, the estimation error is driven to zero using the estimated speed as a feedback ($\tilde{\omega}_m = \omega_m - \hat{\omega}_m$). Sufficiently fast means that the observer has to be 3-5 times faster than the speed PI controller + mechanical plant [3].

$\boldsymbol{L}$ can be designed using the pole placement control approach. The closed-loop poles are placed at the desired place, and the new characteristic equation is calculated. By comparing the coefficients of the new and the old characteristic equations, the gains are found.

In this case, the poles of the new system are placed such as: $s_1 = [-50 - 50j]$, and $s_2 = [-50 + 50j]$. By doing so, the dampening of the system will be $1/\sqrt{2} \approx 0.707$, which will result in a stable (poles are located in the left-hand plane (LHP)), fast observer response with an acceptable overshoot [3]. Pole placement is a valid method here because the observer is a mathematical construction, thus limiters will not impose problems.

The overshoot of the observer is reduced by increasing the damping of the observer.

For the given system, the calculated observer gains are the following:

$$\boldsymbol{L} = \begin{bmatrix} 100 & -73 \end{bmatrix}' \tag{21}$$

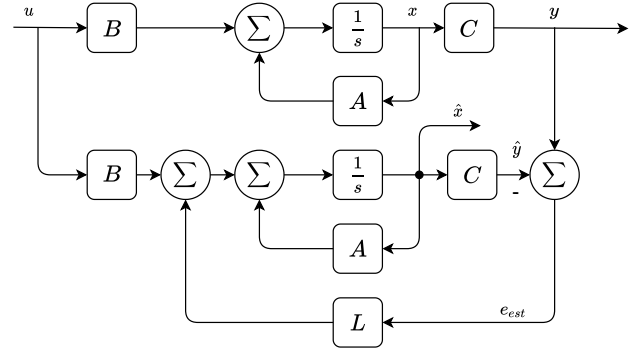The block diagram of the state observer is shown in figure 3.

Figure 3: *Structure of the Luenberger Load Observer*

3.2 Discrete Luenberger Observer

The observer in the above discusses form is continuous which is obviously a problem. This subsection gives a simple solution to this problem. The estimator matrices are re-formulated using the now available observer gain $\boldsymbol{L}$.

Using figure 3, one can conclude that the new system matrices are the following:

$$A_{est} = A - LC$$
$$B_{est} = \begin{bmatrix} B & \boldsymbol{L} \end{bmatrix}$$
$$C_{est} = \begin{bmatrix} 1 & 0 \\ 0 & 1 \end{bmatrix} \tag{22}$$
$$D_{est} = 0$$

Then, using the new matrices from (22), a new observer structure can be acquired. This is shown on figure 4. Discretization of the matrices using the MATLAB command 'c2dm' yields the observer in discrete form.
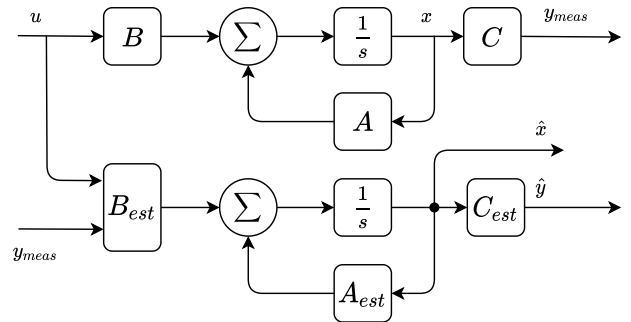

Figure 4: *Structure of the Kalman-filter*

3.3 Kalman-filter

aaa

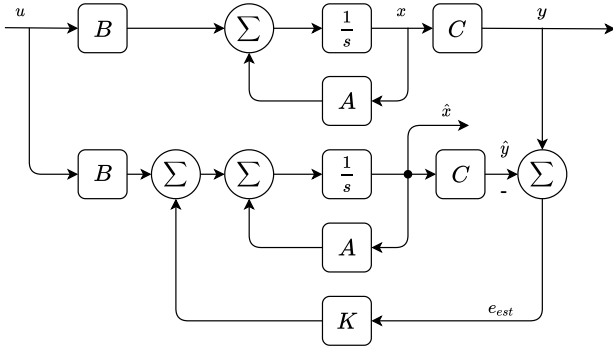The cost function is defined such as ... [6] 5

Figure 5: *Structure of the Kalman-filter*

3.4 Discrete Kalman-filter

The previously introduced discretization of the observer can be redone here too. This is shown on figure 6. The system matrix is calculated such as:
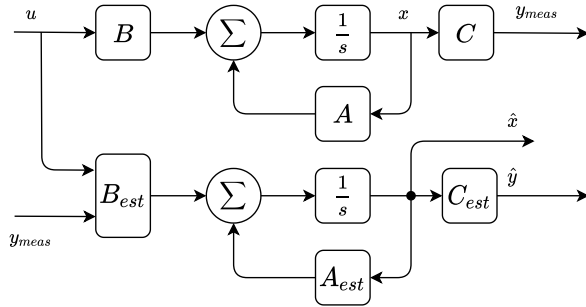
$$A_{est} = A - KC \quad (23)$$

Figure 6: *Structure of the Discrete Kalman-filter*

4 SIMULATION RESULTS

This section shows and discusses the simulation results of the modeled load estimators defined in Section 3. The base of all simulations and thus experiments is the system introduced in Section 2.

The gains of the FOC PI controllers defined above are held constant unless noted otherwise. The parameters for those two controllers are shown in table 2 and they are chosen based on report [1].

Table 2: *System parameters, from previous projects such as*

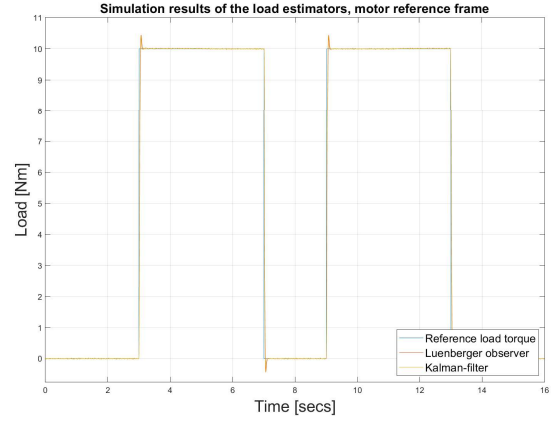| Description	Notation	Value	Unit
q-axis proportional gain	Kp_q	3.8	-
q-axis integral gain	Ki_q	463	-
d-axis proportional gain	Kp_d	3.8	-
d-axis integral gain	Ki_d	463	-
Speed proportional gain	Kp_{speed}	0.4	-
Speed integral gain	Ki_{speed}	1.2	-
Anti-windup gain	$K_{as,PM}$	5	-

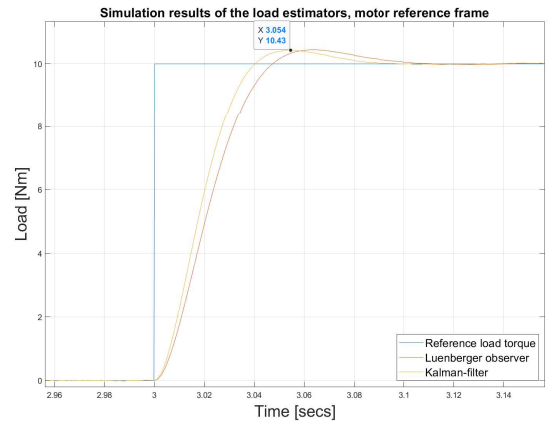Figure 7: *Comparison of the estimated load signals*

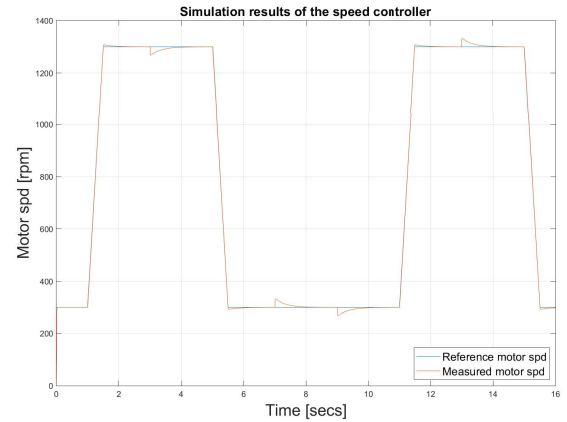Figure 8: *Comparison of the estimated load signals - zoomed-in*

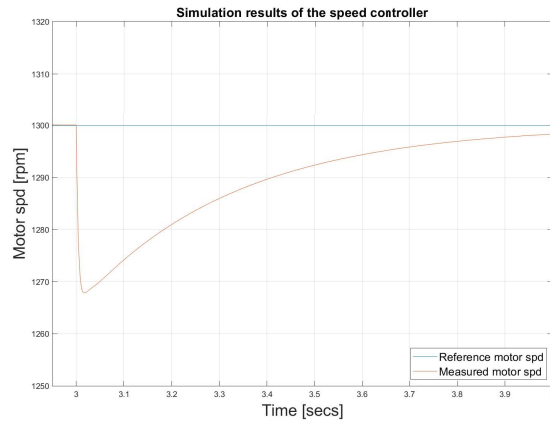Figure 9: *Speed ctrl, transient response in simulation, feed-forward compensation disabled*

Figure 10: *Speed ctrl, transient response in simulation, zoomed-in, feed-forward compensation disabled*
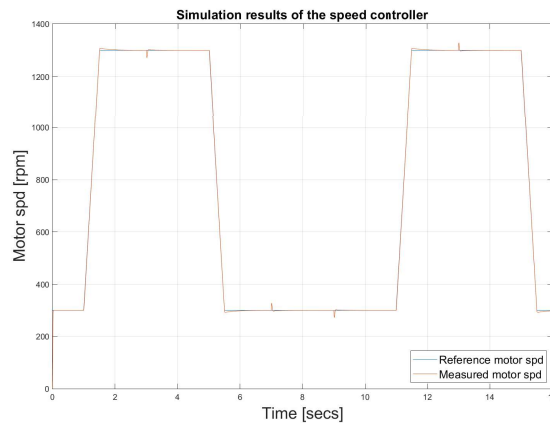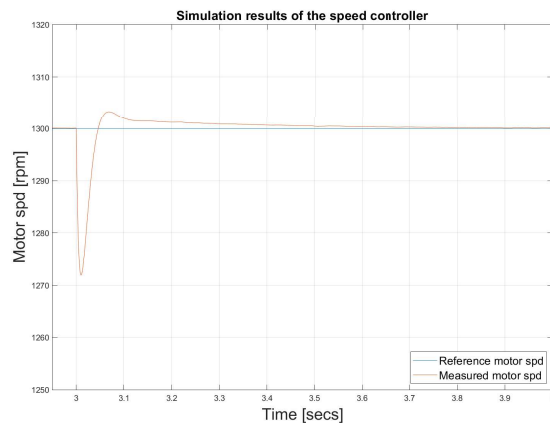
5 CONCLUSION

aaa

REFERENCES

[1] B. Temesi, U. G. Gautadottir, *Sensorless Control of PMSM Drive Using Sliding-Mode-Observers*   AAU, Denmark, 2020 Master's thesis.

[2] D. Wilson, *Motor Control Compendium*, 1st-ed   . 2011

[3] C. L. Phillips, and R. D. Harbor, *Feedback Control Systems*   4th Edition. New Jersey: Prentice Hall, 2000, ISBN: 0-13-949090-6.

[4] K. Lu, *Control of Electrical Drive Systems and Converts Lecture 1 Slides*, 1st-ed   . pp. 1-30, 2019

[5] Z. Kuang, B. Du, S. Cui, and C. C. Chan, *Speed Control of Load Torque Feedforward Compensation Based on Linear Active Disturbance Rejection for Five-Phase PMSM*   in IEEE Access, vol. 7, pp. 159 787–159 796, 2019, ISSN:21693536. DOI: 10.1109/AC-CESS.2019.2950368.

[6] Dan Simon, *Optimal State Estimation*   2006, John Wiley and Sons, Inc. ISBN: 13-978-0-471-70858-2

Figure 11: *Speed ctrl, transient response in simulation, feed-forward compensation enabled*

Figure 12: *Speed ctrl, transient response in simulation, zoomed-in, feed-forward compensation enabled*